Characterisation of mesosegregations in large steel ingots

Lucie Gutman, J.R. Kennedy, François Roch, Arthur Marceaux Dit Clément, Lise Salsi, Jean Cauzid, Bernard Rouat, Hervé Combeau, Miha Založnik, Julien Zollinger

Preprint version of published article. Cite as:
L. Gutman et al., Characterisation of mesosegregations in large steel ingots,
IOP Conference Series: Materials Science and Engineering, **in press** (2022)

Characterisation of mesosegregations in large steel ingots

L Gutman[1,2], J R Kennedy[2], F Roch[1], A Marceaux dit Clément[1], L Salsi[3], J Cauzid[3], B Rouat[2], H Combeau[2], M Založnik[2] and J Zollinger[2]

[1] Framatome DTI, F-92400 Courbevoie
[2] Université de Lorraine, CNRS, IJL, F-54000 Nancy
[3] Université de Lorraine, CNRS, GeoRessources, F-54000 Nancy

Abstract. The chemical composition mapping of low-alloyed steel ingots used for the nuclear industry is crucial in the manufacturing of forgings and their final quality mastering. Mechanical properties of forged and hot-rolled steels may be affected by chemically segregated bands. These bands arise from segregations that appear at the scale of a few grains in the as-cast structure: the so-called mesosegregations. While segregation at the scale of dendrite arms (microsegregation) and the scale of the casting (macrosegregation) is well understood and can be readily characterized, only little is known about the formation of mesosegregation. The first step towards understanding the cause behind mesosegregation formation can be brought through comprehensive chemical characterisation at the scale of several grains (mesoscopic scale), which requires using different characterisation techniques compared to micro- or macrosegregation characterisation. We developed a sampling and characterisation methodology that allows segregations to be mapped at the mesoscopic scale using micro X-ray fluorescence (μXRF). Characterisation technique, sampling methodology, and sample size must be adapted to consider the different solidification structures; both at smaller (dendrite arms, grains) and larger (macrostructure) scales. Segregations were characterised on a 113 x 98 mm² steel plate extracted from a low-alloyed steel large ingot.

1. Introduction

Segregation of alloying elements occurs as steel solidifies. In steel, the common alloying elements (C, Mn, Mo for instance) are more soluble in the liquid than in the solid [1]. As steel solidifies, alloying elements are rejected into the liquid phase. This solute enrichment of the liquid phase leads to chemical heterogeneity in the solid-state. Such heterogeneity is called segregation and exists at different scales. Segregation is a departure from the nominal chemical composition of the steel, local enrichments cause positive segregations whereas local depletions cause negative segregations. *Microsegregation* is segregation observed at the dendrite scale (from μm to a few hundreds of μm), due to solute rejection during the growth of dendrites. It can be influenced by solute diffusion difference between the liquid and solid-state [2]. Microsegregation creates depleted solid and enriched liquid that move at the ingot scale (m) through convection, movement of grains, solidification shrinkage and mushy zone deformation forming *macrosegregation* [3]. While heat treatment can reduce microsegregation through diffusion, macrosegregation cannot be reduced at the industrial scale since diffusion is too slow of a process. Thus macrosegregation cannot be reduced after solidification, it may remain in the semi-products and even in the forged part thus affecting final mechanical properties [4].

Segregations that exist in the ingot influence solid-state transformations, which cause heterogeneities in microstructures and final mechanical properties. Forging steps change the size, shape, and distribution of segregations but do not decrease their intensity or number [5]. The change in shape and size of segregations causes a banding phenomenon in forged and hot-rolled steels: bands of different microstructures and compositions are observed [6]. Banding in steel leads to anisotropic mechanical

properties. This is especially true for impact toughness properties which can be sensitive to orientation and depth of specimen sampling [7, 8]. Banding is caused by segregations larger than the dendrite scale (microsegregations), but smaller than channels (macrosegregation) [9]. Such intermediate scale segregations, probably at the grain-scale, are called *mesosegregations*. To understand and influence banding phenomena, understanding the formation of mesosegregations is key.

A comprehensive characterisation of mesosegregations is the first step towards understanding their formation. Different characterisation techniques exist to track chemical heterogeneities at different scales. Investigation of microsegregation is commonly carried out with an Electron Probe Micro Analyser (EPMA) which enables the quantification of the chemical composition with an interaction volume of roughly 1 μm^3. In large steel ingots, macrosegregation can be tracked with Optical Emission Spectrometry (OES) or infrared combustion analysis for carbon and sulphur investigation. Macrosegregation can also be detected by X-Ray Fluorescence (XRF) spectroscopy. Manganese (Mn) and Molybdenum (Mo) macrosegregation patterns can easily be distinguished, with a 5 mm analysis step and minimal sample preparation [10]. However, these techniques cannot be adapted to intermediate-scale segregation in the case of large ingots due to their lack of spatial resolution. Large ingots used in the nuclear industry have long solidification times and so present large structures: investigated samples present secondary arm spacing of 800 µm. Hence to investigate the occurrence of mesosegregations in such ingots, chemical composition should be mapped at the centimetric grain scale. At this scale, EPMA analysis is impractical: too detailed and too time consuming. In contrast, the OES and combustion analysis techniques are too coarse to be implemented at a centimetric scale.

In this paper we developed a new sampling and characterisation methodology, suitable for the chemical analysis of mesosegregations in steel ingots. This new method is based on micro-X-Ray Fluorescence (µXRF), which has begun to be investigated as a tool to analyse centreline segregation during continuous casting [11, 12]. First, the effects of sampling on the observed structures and recorded data were analysed in order to define sampling parameters applicable to a centimetric scale mapping. Then, calibration was conducted by comparison with EPMA to convert X-ray counts to quantitative concentration. Finally, a centimetric scale quantitative map was produced combining µXRF and EPMA calibration.

2. Material and methods

2.1. Samples

The low-alloy steel 16MND5 (0.16 %wt. C, 1.45 %wt. Mn, 0.725 %wt. Ni and 0.5 %wt. Mo) was selected for analysis. Samples were taken from the equiaxed region of an industrially produced 116 ton directionally solidified ingot. Samples were cut using wire electron discharge machining.

2.2. Micro-X-Ray Fluorescence (µXRF)

Micro-X-Ray Fluorescence (µXRF) analyses were performed with a Bruker M4 Tornado device equipped with a Rh X-ray source (30 W power). Two EDS (Energy Dispersive Spectroscopy) detectors are located on either side of the primary X-ray source. Both the source and the detectors are fixed in the vacuum chamber (20 mbar vacuum) whereas the samples are placed on a motorized stage. The spot size focused on the sample is 20 µm.

Low-alloyed steel samples of different sizes were used to investigate the effects of experimental conditions on the results. For µXRF measurements, a metallographic surface finish is not required, samples were ground flat with Si-C paper down to P800 (21.8 µm granulometry).

Concerning the primary X-ray source conditions, acceleration voltage, current, and the use of filters on the beam enable improvement of the signal and minimisation of artefacts. An indicator for artefact minimisation is the dead time, as dead time approaches 20 %, artefacts are minimised. Dead time can be managed by balancing current, acceleration voltage, and filters. Acceleration voltage was set to 50 keV for all analyses. Filters used on the X-ray beam are high-pass filters, they enable suppression of a part of the signal to avoid saturation and artefacts. However, strong filters can suppress peaks that correspond to elements of interest, for instance, the Manganese signal is affected by such strong filters.

The use of filters can be optimised to approach 20 % of dead time without decreasing the current. This is beneficial as a low current leads to a weak outcoming signal.

2.3. Electron Probe Micro Analyzer (EPMA)

The Electron Probe Micro Analyser (EPMA) device used is a JEOL JXA-8530F equipped with a FEG source, an EDS and 5 WDS (Energy and Wavelength Dispersive Spectroscopy) detectors. The electron beam operates at 20 kV and 100 nA for the analysis of Mn and Mo on LIF and PET crystals respectively, calibrated with standards Pel6080-Mn and Pel6080-Mo. Samples analysed with EPMA require a mirror-like surface and were polished with a 1µm diamond slurry.

2.4. Cumulative solid fraction curves

As solidification occurs the solute concentration in liquid increases (the partition coefficients of the studied elements are smaller than one). One way to compare the different characterisation techniques is to associate a solid fraction with data points and to plot the evolution of concentration (for EPMA analysis) or peak intensity (for µXRF analysis) as a function of the increasing solid fraction. The first solid to form is the most depleted and the last solid to form is the richest in solute. Intermediate data points are then ranked. Different ranking techniques exist and are used for microsegregation analysis, several of them are compared by Ganesan [13]. In the present study, the data points are arranged monotonically into ascending order according to a single element (Flemings-Grungor method).

3. Experimental methodology development

3.1. Sampling effect

The X-ray beam of the µXRF device used in this study has a 20 µm width with a fixed focal point. With µXRF the sampling is not homogenous in both directions. The surface is scanned continuously in the *x*-direction, a single spectrum is obtained by collecting X-rays over a given time, as the stage translates at a constant speed this corresponds to a specific length, called the analysis step. In the *y*-direction, the scanning is discrete since the lines are spaced by a distance equal to the analysis step in order to maintain square pixels. A certain area between the lines, corresponding to the difference between the analysis step and the beam width (20 µm) is not analysed, as shown in the schematic in figure 1. The only way to map the whole surface is to use an analysis step equal to the beam width, 20 µm, in which case, there is no space between the analysed lines.

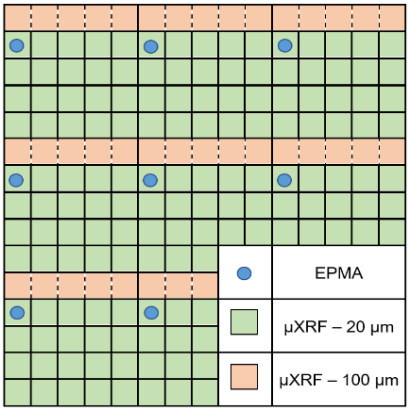

Figure 1. Schematic of the surface scanning during µXRF analysis with different analysis steps. When the analysis step is 100 µm, a band of 80 µm is not analysed between each analysed line of 20 µm width. The EPMA grid discussed in paragraph 3.2 is also represented.

To investigate the effect of the analysis step and time on segregation mapping, the same sample was mapped in similar experimental conditions but with different analysis steps sizes. The tests were performed on a 4.4 x 5.6 mm² zone. The stage speed was kept constant for each test, the primary X-ray source was unfiltered with a 50 keV acceleration voltage and 200 µA current, only the analysis step and the associated analysis time changed. Five different configurations were tested (notation: analysis step_analysis time): 20µm_20ms, 50µm_50ms, 100µm_100ms, 150µm_150ms and 200µm_200ms.

Preprint version of published article. Cite as:
L. Gutman et al., Characterisation of mesosegregations in large steel ingots,
IOP Conference Series: Materials Science and Engineering, **in press** (2022)

Three representative maps are presented in figure 2. The visual aspects of the maps are affected by the sampling. With a 20 µm step, the surface is completely mapped, the edges of the structures are sharp, small microstructure details are detected. As the acquisition step increases, the structures seem to spread out and their shape can be distorted. With acquisition steps bigger than 100 µm the shape of the structure is no longer representative, as such, acquisition steps smaller or equal to 100 µm should be favoured.

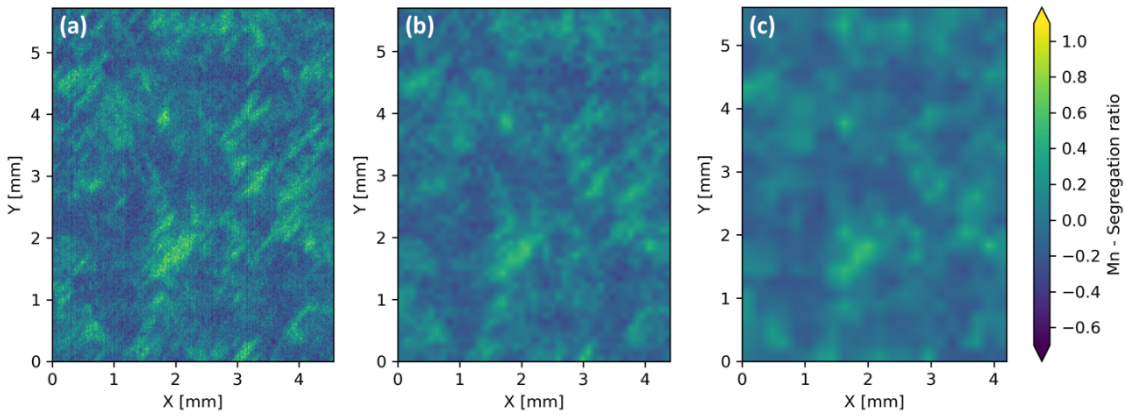

Figure 2. Maps of Mn segregation ratio of a sample 4.4 x 5.6 mm² analysed with µXRF (X-ray beam: unfiltered, 50 keV, 200 µA) with different analysis step and time ((a) 20µm_20ms, (b) 100µm_100ms (c) 200µm_200ms).

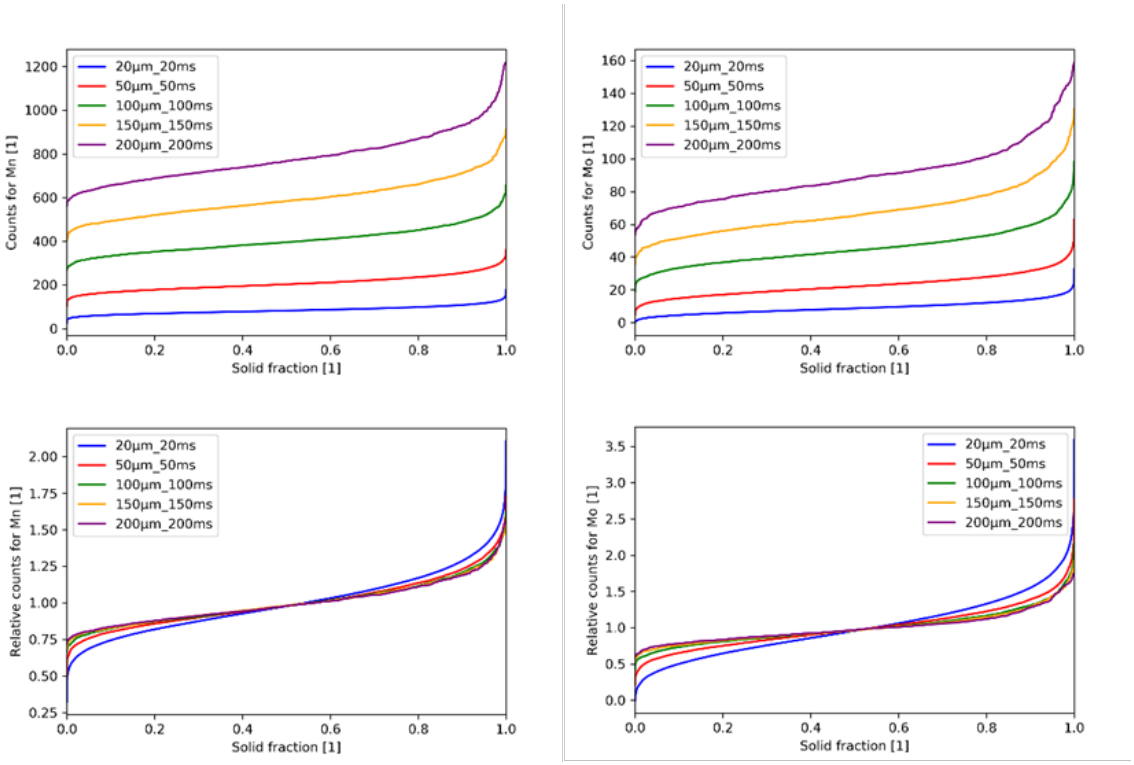

Figure 3. Classic (top) and relative (bottom) cumulative solid fraction curves (peak intensity as a function of the solid fraction) for µXRF data collection on a sample 4.4 x 5.6 mm², in the same experimental conditions (unfiltered, 50 keV, 200 µA) but with different analysis step and time (20µm_20ms, 50µm_50ms, 100µm_100ms, 150µm_150ms and 200µm_200ms). On the left is Mn peak intensity, on the right is Mo peak intensity.

The cumulative solid fraction curves are presented for Mn and Mo in figure 3. The collected peak intensity increases with the analysis step for both elements. It is linked to an increase in acquisition time: the longer the detector collects the fluorescent X-rays, the greater the peak intensity. The intensity of the peaks corresponds to the acquisition time, but the curve shape is linked to the acquisition step. To isolate the influence of the acquisition step relative cumulative solid fraction curves are used. With a step of 20 µm, the whole surface is analysed whereas in the other cases it is not. The curves associated with analysis steps of 100 µm, 150 µm, and 200 µm are very similar. Increasing the analysis step does not seem to decrease the quality of the information needed for solid fraction curves. The benefit of small analysis steps such as 100 µm is questionable: it is time-consuming, and a 200 µm step can provide the same information. Using a small step can however be justified if mapping is of interest rather than cumulative segregation curves.

3.2. Quantification

µXRF analysis can provide chemical composition mapping at a centimetric scale. However, the initial map is expressed in counts, which correspond to the intensity of the peak associated with the element, and not its concentration itself. EPMA analysis, on the other hand, can provide quantified local concentrations, but cannot be used at a large scale. By combining these techniques, the µXRF centimetric scale mapping can be quantified.

To quantify the µXRF analysis, a 400-point grid of EPMA spot analyses were conducted on 3 different samples. A step size of 100 µm was used, hence the surface analysed was 1.9 x 1.9 mm². The same samples were then analysed with µXRF using the same experimental conditions as the centimetric mapping to be quantified. EPMA and µXRF data points were ranked in ascending order, then assuming that the greatest peak intensity corresponds to the greatest concentration and vice versa, EPMA data was plotted against µXRF data and a linear regression was performed on the curve. The regression equation can be applied to convert the peak intensities to concentrations.

3.3. Quantitative centimetric scale mapping

Based on previous observations, experimental conditions were defined to perform centimetric scale mapping. The analysed surface was 113 x 98 mm², the acquisition steps were 100 µm in both directions (resulting in 1 109 511 analysis points) and the analysis time was 45 ms per spectra. The X-ray beam operated at 50 keV and 200 µA, and a 100 µm thick Al filter was used to reduce dead time to 21 %. Once the data was collected, the quantification method was applied and quantitative centimetric scale maps obtained. The quantified map for Mn is presented in figure 4.

Mn is rejected into the liquid phase during solidification. Dendrite trunks and secondary arms can be distinguished on the quantified map. At the centimetric scale, the structures do not appear distorted confirming that our developed analysis protocol is suitable. The microsegregation is visible on the centimetric scale map. At a larger scale, two round spots of a few millimetres can be observed near the centre and at the bottom left corner of the map on both maps, which may be channel segregates. Also, the interdendritic spaces on the top right side of the map seem richer in Mn than in the centre of the map.

4. Conclusion

The understanding of mesosegregation formation requires chemical analysis at a centimetric scale. The objective of this work was the development of a new sampling and characterisation methodology that relies on µXRF and allows centimetric scale mapping. First, the effect of sampling on the observed structures was investigated to select suitable experimental conditions for centimetric scale mapping. As the surface scanning with µXRF techniques is anisotropic, a small acquisition step is employed to avoid shape distortion of the structures (it should be smaller or equal to 100 µm). The chemical composition of a 113 x 98 mm² sample was mapped with a 100 µm analysis step with the µXRF technique and quantified by calibration with EPMA. The chemical composition mapping reveals microsegregations and chemical heterogeneities at a larger scale. A geostatistical approach should be used on centimetric scale mappings to investigate mesosegregations patterns.

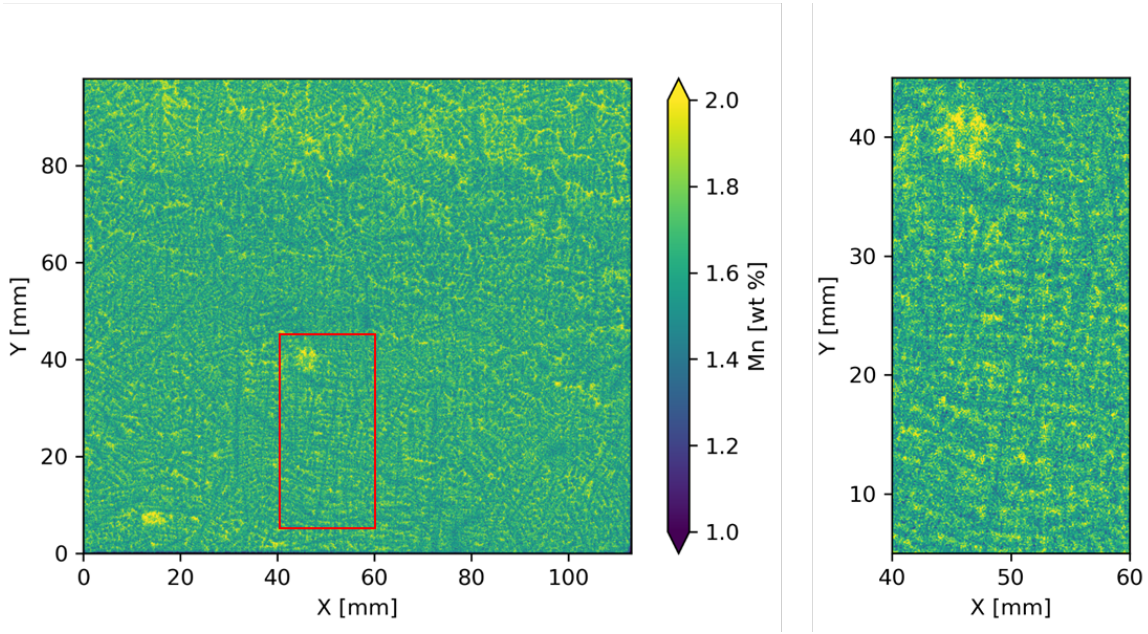

Figure 4. Map of Mn realised on a 113 x 98 mm² sample analysed with µXRF (X-ray beam: Al-100 µm, 50 keV, 200 µA), with a 100 µm analysis step and 45 ms of acquisition time per spectra. An enlarged view of the area delimited in red is shown on the right.

Acknowledgments
This research work is supported by ANRT France under a CIFRE Ph.D. fellowship (Grant Number 2020/1234) and through the Industrial chair *Solidification* at Institut Jean Lamour, supported by ArcelorMittal, ArcelorMittal Industeel, CEA, EDF and Framatome.

References
[1] Lesoult G 1986 *Techniques de l'ingénieur. Matériaux métalliques.* **M58** 1
[2] Dantzig J A and Rappaz M 2009 *Solidification*. (Lausanne: EPFL Press) p 394
[3] Pickering E J 2013 *ISIJ international.* **53** 935–49
[4] Ludwig A, Wu M and Kharicha A 2015 *Metall. Mater. Trans. A* **46** 4854–67
[5] Thornthon P A and Colangelo V J 1976 *Metall. Mater. Trans. B.* **7** 425–33
[6] Pickering E J and Bhadeshia H K D H 2014 *J. Press. Vessel Technol. Trans. ASME.* **136**
[7] Salimi A, Zadeh H M, Toroghinejad M R, Asefi D and Ansaripour A 1996 *Materiali in tehnologije.* **47** 385
[8] Hong S, Song, J, Kim MC, Choi KJ and Lee BS 2015 *Met. Mater. Int.* **22** 196–203
[9] Yamashita T, Torizuka S and Nagai K 2003 *ISIJ international.* **43** 1833–41
[10] Pickering E J and Holland M 2014 *Ironmaking & Steelmaking.* **41** 493–9
[11] Sengupta J, Leung J and Noorafkan A 2017 *AISTech 2017 Proceedings.* (Warrendale: AIST) p 1925
[12] Sengupta J and Noorafkan A 2018 *AISTech 2018 Proceedings.* (Warrendale: AIST) p 2637
[13] Ganesan M, Dye D and Lee P D 2005 *Metall. Mater. Trans. A.* **36** 2191–204